Stimulation of Directed Bone Growth at Oxidized Titanium Implants by Macroscopic Grooves: An In Vivo Study

Jan Hall, MSc;* Patricia Miranda-Burgos, DDS;† Lars Sennerby, DDS, PhD†

ABSTRACT

Background: The influence of thread design at the millimeter level and surface topography at the micrometer level on bone integration and the stability of dental implants have been studied extensively. However, less is known about the influence of implant structures in the range of 50 to 200 μm.

Purpose: The present in vivo investigation was undertaken to study if bone formation and implant stability were influenced by 110 (S1) and 200 (S3) μm–wide and 70 μm–deep grooves positioned at a thread flank of oxidized titanium implants.

Materials and Methods: Eighteen rabbits and oxidized titanium implants (3.75 mm in diameter and 7 mm long) were used in the study. Nine rabbits received three control implants and three test implants with a 110 μm–wide groove added to one thread flank. The remaining nine rabbits received three control implants and three test implants with a 200 μm–wide groove. The animals were followed for 6 weeks. Removal torque (RTQ) tests were applied to two of the implants in each leg. The remaining implant per leg was retrieved for histology. The degree of bone fill within the grooves and corresponding bone formation at the opposing surfaces, the bone area within the threads, and the degree of bone-implant contact were calculated for each implant.

Results: The histologic analyses revealed an affinity for bone formation within the grooves. The RTQ tests showed that the peak RTQ was approximately 30% higher for the S1 implants compared with control implants without a groove. The difference was statistically significant ($p < .05$) for tibial and pooled implants. A similar but smaller and not statistically significant effect, approximately 8%, was measured for the S3 implants. The histomorphometric measurements confirmed the observed affinity of bone for the grooves. For S1 implants, 78.7 ± 15.8% of the grooves were filled with bone, whereas only 46.2 ± 27% of the corresponding flank surface showed the presence of bone ($p < .05$). The corresponding figures for S3 and control implants were 72.7 ± 25.1% and 48.5 ± 13.6%, respectively ($p < .05$). The degrees of bone-implant contact and bone area within the threads were similar for test and control implants.

Conclusion: It is concluded that 110 and 200 μm–wide and 70 μm–deep grooves at oxidized implant surfaces stimulated bone to preferentially form within and along the groove in the rabbit model. The 110 μm–wide groove was shown to increase the resistance to shear forces significantly. It is suggested that implants with such a groove may be one way to optimize implant stability in suboptimal clinical conditions.

KEY WORDS: experimental study, histology, removal torque

Threaded titanium implants have been extensively used as anchorage units for dental prostheses in the rehabilitation of edentulous patients. The documented good clinical long-term outcome, including minimal marginal bone resorption,[1] indicates that the threaded design allows for optimal or near-optimal distribution of mechanical forces in the surrounding bone. Today most commercially available implants have a thread profile in the low-millimeter range. In addition to the threaded design, topographic modifications of the implant surface at the micrometer level are also applied extensively to commercial implants. The modified topography often results in a larger surface area that provides increased mechanical retention in bone. When implants with rough sandblasted/acid-etched or porous

*Nobel Biocare AB, Göteborg, Sweden; †Department of Biomaterials, Institute of Surgical Sciences, Sahlgrenska Academy, Göteborg University, Göteborg, Sweden

Reprint requests: Jan Hall, Nobel Biocare AB, PO Box 5190, SE 402 26 Göteborg, Sweden; e-mail: jan.hall@nobelbiocare.com

titanium oxide surfaces have been compared with relatively smooth turned titanium implants in experimental studies, the level of osseointegration has been reported to be higher for the roughened-surface implants.[2–6] Implant surfaces modified by anodic oxidation[7] have demonstrated a more rapid bone integration[8–10] and a higher resistance to shear forces[11,12] compared with nonmodified control surfaces. These data suggest that the surface structures in the micrometer range have a positive influence on implant integration kinetics and stability. Recent clinical studies have, in fact, indicated a better performance of oxidized implants than machine-turned ones when subjected to immediate loading in soft bone qualities[13–16] and in grafted bone.[17] However, additional improvements in implant properties are necessary to further increase the predictability of implant treatment in non–optimal bone situations. In search of such improvements it may be interesting to study implant structures in the range of 50 to 200 μm, which are between the sizes of the extensively studied typical thread geometries and surface topographies. Such structures have often been overlooked in investigations on threaded dental implants.

Structures in the range of hundred micrometers to millimeters have been studied on nonthreaded orthopedic devices and dental implants.[18] Often metallic fibers, beads, or balls were sintered onto the implant surface to give a three-dimensional porous structure with a thickness of a few hundred micrometers. It was shown that ingrowth of vascularized bone into the sintered three-dimensional structures depended on the pore size, which had to be larger than a threshold value of approximately 100 μm. Bone could then grow into the porous structures and allow for mechanical interlock of the implants, provided that the implants could be inserted with sufficient initial stability. Recently, Hyung-Seung Ryu and colleagues observed osteoconduction in linear pore channels, which were only 50 μm in diameter.[19] Scanning electron microscopic studies of the interface between a porous implant surface and bone have shown that bone can grow into pores only a few micrometers wide.[20] Such findings indicate that bone can grow into structures with arbitrary pore diameter or width and penetration depth provided that the width and depth are within the same order of magnitude.

It has also been shown that smaller structures in the micrometer range could influence cellular response in vitro. Boyan and colleagues showed that forces acting on cells as they migrated on topographically modified surfaces stimulated matrix production.[21] In vitro studies on surfaces with grooved structures in the range of tens of micrometers showed that it was possible to promote directed cell migration.[22–26] It was concluded that grooves with dimensions similar to the size of the cells studied could stimulate cell migration within the grooves, whereas significantly larger or smaller grooves had negligible effects on the cells. It seems that forces given by the geometric groove boundaries determined cell configuration and response in such in vitro systems. However, it is not unlikely that forces given by motion of fluids may have stronger effects on cell response in in vivo systems.

The present in vivo investigation was undertaken to study if it was possible to stimulate bone formation within 110 or 200 μm–wide and 70 μm–deep grooves positioned at the thread flank of oxidized titanium implants. Thus, the groove dimensions were clearly larger than the size of bone-forming cells, and the extension of the grooves was several orders of magnitude larger than their width and depth. Our hypothesis was that bone could be directed to grow along such grooves and that the bone formation within the groove could significantly increase implant stability.

MATERIALS AND METHODS

Animals and Anesthesia

Eighteen adult New Zealand White female rabbits were used in the study, which was approved by the local animal ethics committee. Surgery was performed under sterile conditions. General anesthesia was induced by intramuscular injections of a fluanisone-fentanyl blend (0.7 mL, Hypnorm™, Helsingborg, Sweden) and intraperitoneal injection of diazepam (0.25 mg/kg, Apozepam™, Alpharma AB, Stockholm, Sweden). Local anesthesia was induced at both proximal tibial metaphyses and distal femoral condyles by injections of lidocaine (about 2 mL, Xylocaine®, AstraZeneca AB, Södertälje, Sweden).

Implants, Surgery, and Experimental Protocol

Threaded titanium implants (7 mm long, 3.75 mm in diameter, TiUnite™, Mk III, Nobel Biocare AB, Göteborg, Sweden) were used in the study. The implants were manufactured without the apical self-tapping feature in order not to influence the results from the removal torque mea-

surements described below. All implants had a surface made by anodic oxidation (TiUnite), which has been described in detail.[7] In brief, the surface comprises a highly crystalline titanium oxide and a porous structure with pore sizes from the low-submicrometer range to 10 μm.

Prior to oxidation, two groups of test implants had a single groove positioned at the center of the superior thread flank, that is, facing the head of the implant. The grooves were 70 μm deep and 110 (S1) or 200 (S3) μm wide, respectively (Figure 1). Implants without grooves were used as controls.

Three test and three control implants were placed in each rabbit. One side was used for control implants, and the contralateral side was used for test implants. One implant was positioned in the femoral condyle and two implants were positioned in the tibial metaphysis. Nine rabbits received S1 ($n = 27$) and control ($n = 27$) implants and nine rabbits received S3 ($n = 27$) and control ($n = 27$) implants. The experimental sites were opened via incisions through skin and fascia, and the bone surfaces were exposed with the aid of an elevator. The implants were placed after preparation with 2.0 and 3.0 mm twist drills followed by screw tapping. The wounds were closed by suturing of fascia and skin.

After a healing period of 6 weeks, the animals were anesthetized as described above. The animals were then sacrificed by an overdose of anesthesia. The femoral implants and the distal implants in the tibial metaphyses were subjected to removal torque (RTQ) tests. The RTQ tests were performed in a specially designed rig using a motor-driven device. The implants had a special internal geometric feature and a connector (Stargrip™, Nobel Biocare AB) to ensure a firm grip between the implant and the connector. A linearly increasing torque was applied until failure of integration was reached, and the peak value in newton-centimeters was recorded. The remaining implants were retrieved for histology.

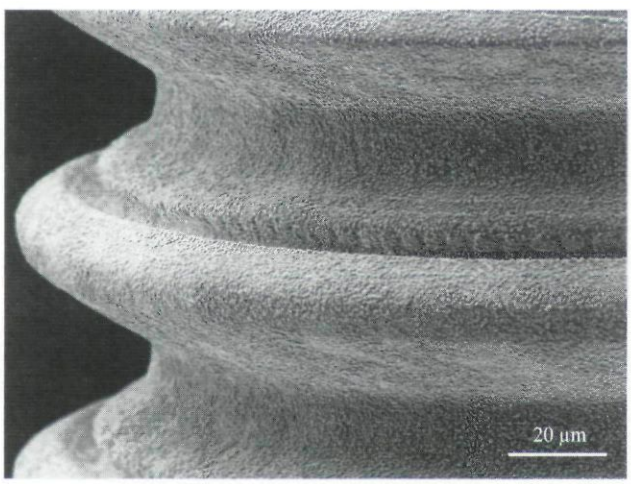

Figure 1 Scanning electron microscopic image of an oxidized implant with a groove on the thread flank.

The fixated specimens were dehydrated in a graded series of ethanol and embedded in light-curing methacrylate (Technovit® 7200 VCL, Heraeus Kulzer GmbH & Co., Wehrheim, Germany). Ground sections, approximately 10 μm thick, were prepared using a sawing and grinding technique (EXAKT Apparatebau GmbH & Co., Norderstedt, Germany). The sections were cut in the direction parallel to the implant axis. The sections were stained with toluidine blue.

Examinations were performed in a Leitz microscope equipped with a Microvid® system (Ernst Leitz GmbH, Wetzlar, Germany) for morphometric measurements. The presence of bone in the groove and on the corresponding opposing flank surface was quantified within each implant thread. The bone area filling the space between the implant threads and the degree of bone-implant contact were also calculated.

Statistics

The Wilcoxon signed rank test was used to calculate possible differences between test and control implants. A statistically significant difference was considered if $p < .05$.

RESULTS

All animals recovered after surgery, and healing was uneventful.

The $(SX - C_{SX})/C_{SX}*100$ value (Table 1), which describes the mean value of the percent difference between each pair of test and control implants from each rabbit, showed that the measured peak RTQ was 30.4% (tibia) and 26.6% (femur) higher for implants with the 110 μm–wide groove (S1) compared with implants without a groove. The difference was statistically significant ($p < .05$) for tibial and pooled implants (see Table 1). A similar but smaller and not statistically significant effect, 8.3% (tibia) and 7.7% (femur), was measured for the 200 μm–wide groove (S3) (see Table 1).

A typical histologic ground section of the tibial implants comprised the implant with two threads penetrating a 1.5 to 2–mm thick cortical layer and with four threads located in bone marrow tissue (Figures 2 and 3). New bone formation and remodeling were evident within, above, and below the cortical layer. Thin rims of

TABLE 1 Results from Removal Torque Measurements

Site	S1	C_{S1}	Difference, %	*p* Value
Tibia	37.3 ± 10.2	30.4 ± 10.5	30.4 ± 33.8	.04
Femur	63.1 ± 17.0	50.6 ± 12.2	26.6 ± 28.1	NS
Pooled	46.7 ± 12.9	37.2 ± 10.2	25.5 ± 21.2	.04
	S3	C_{S3}	Difference, %	*p* Value
Tibia	34.7 ± 10.1	32.3 ± 6.7	8.3 ± 25.8	NS
Femur	63.3 ± 12.8	59.2 ± 12.2	7.7 ± 16.1	NS
Pooled	49.0 ± 10.2	45.8 ± 7.9	7.3 ± 14.6	NS

C = control; NS = not significant.
Mean values in Newton-centimeters and differences in percent $[(Sx - C_{sx})/C_{sx}*100]$.

bone could be seen at the implant surface in the bone marrow compartment. It was obvious that bone formed predominantly within the grooves with no difference between the two sizes (Figure 3 and 4). At a higher magnification, the mineralized tissue within and outside the grooves had an intimate contact with the surface oxide and often contained large osteocyte lacunae and osteocytes (Figure 4). The occasional presence of several cement lines indicated bone formation in several layers by different osteoblast populations. There were no obvious differences between S1 and S3 implants.

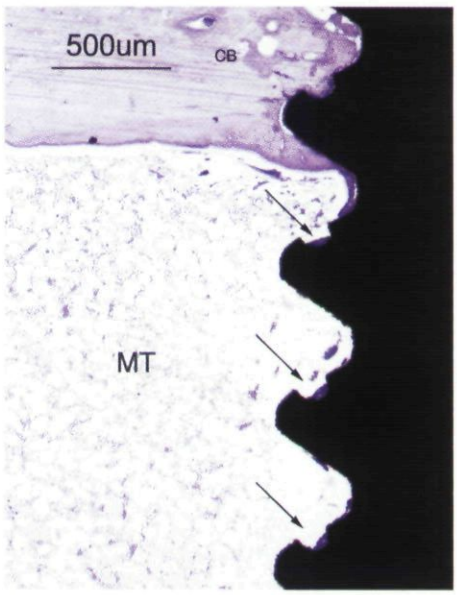

Figure 3 Light micrograph showing an S1 implant after 6 weeks of healing in the rabbit tibia. The groove is clearly visible (*arrows*). Bone is seen in all grooves of this specimen and in the marrow tissue (MT). CB = cortical bone. Bar = 500 μm (stained with toluidine blue and pyronin-G).

The histomorphometric measurements confirmed the observed affinity for bone formation within the grooves. For S1 implants, 78.7 ± 15.8% of the grooves were filled with bone, whereas only 46.2 ± 27% of the corresponding flank surface showed the presence of

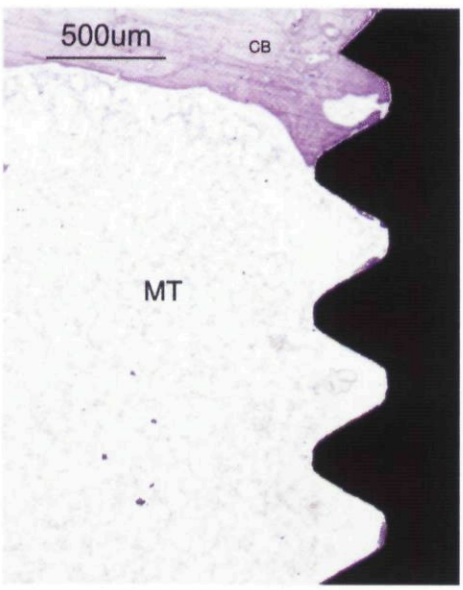

Figure 2 Light micrographs showing a control implant after 6 weeks of healing in the rabbit tibia. The experimental site comprises a thin cortical bone (CB) and marrow tissue (MT). The implant is well integrated with the CB, and thin rims of bone are occasionally seen in the marrow compartment. Bar = 500 μm (stained with toluidine blue and pyronin-G).

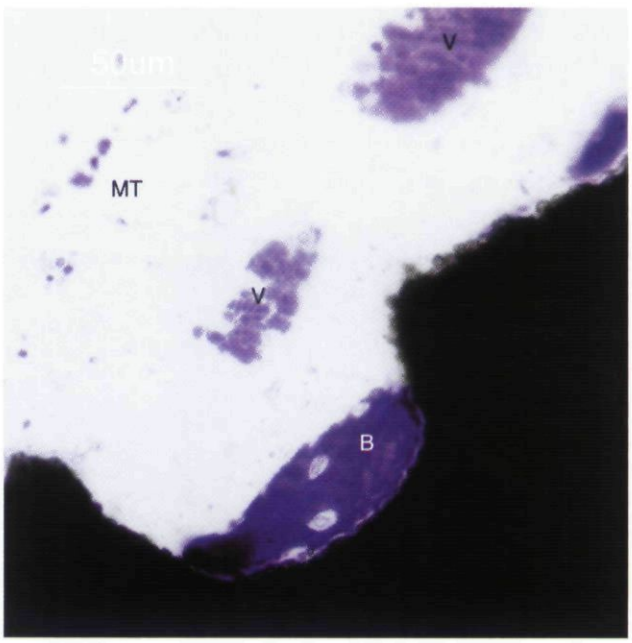

Figure 4 Close-up of Figure 3 showing a thread situated in the marrow compartment. Bone with large osteocyte lacunae is seen in the groove. Bar = 50 μm (stained with toluidine blue and pyronin-G).

bone ($p < .05$) (Figure 5). The corresponding values for S3 and control implants were 72.7 ± 25.1% and 48.5 ± 13.6%, respectively ($p < .05$) (see Figure 5). When analyzing the degree of bone fill at each thread level, it was evident that the difference was greater at threads located in the bone marrow (Figure 6). Similar amounts of bone filling between the threads and similar degrees of bone-implant contact were seen for the S1, S3, and control implants (Table 2).

DISCUSSION

The present experimental study supported the hypothesis that guided bone formation can be stimulated with macroscopic grooves at the thread flank of oxidized titanium implants. The histologic evaluation showed an affinity for bone formation within both 110 (S1) and 200 (S3) μm–wide macroscopic grooves. The biomechanical testing revealed significantly higher resistance to RTQ for the S1 but not for the S3 implants compared with the control implants. The addition of a groove to the thread flank increased the implant surface area by approximately 10% for both S1 and S3 grooves. The increased area may explain the measured increased RTQ for the S3 implants if assuming that the fracture created by the removal force was at the bone/implant interface. The high torque values for the S1 groove suggest that, in this case, bone fractured close to the groove entrance in the plane of the thread flank, which also was demonstrated in a recent rabbit study.[27] Furthermore, the up to 30% increase in implant RTQ suggests that the bone within the groove had matured to significant mechanical strength after 6 weeks from implant insertion.

A clinical dental implant is subjected to loading in axial, lateral, and rotational directions. The ability of an implant to withstand loads and stresses plays an important role in bone tissue response during healing and functional loading. Although the rabbit tibia is not an entirely relevant model for dental implants in clinical function, it is believed to be a relevant model for comparison of the resistance of implants to shear forces. Therefore, it is assumed that the up to 30% increase in the measured RTQ may significantly contribute to clinical implant stability, especially in cases with compromised bone.

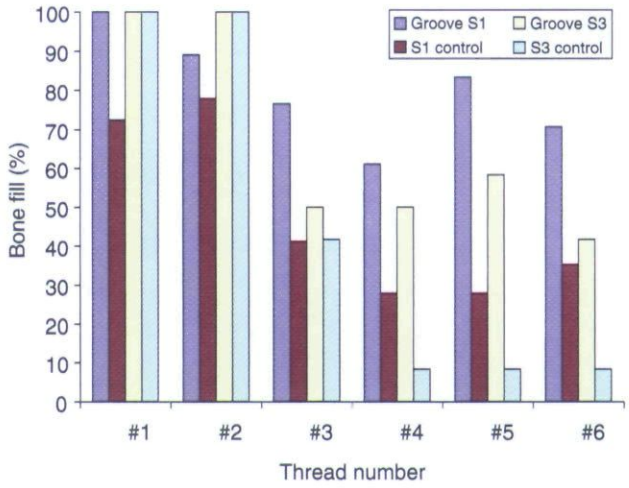

Figure 6 Graph showing bone fill in grooves and opposing surfaces for each thread level. Threads 1 and 2 were usually in the cortical layer, and the remaining threads were in the marrow cavity.

The histologic analysis after 6 weeks of healing revealed bone tissue formation and remodeling at the implant threads located in and near the cortical layer. Bone formation was also seen at the implant surface located in the marrow compartment, usually as solitary islands with apparently no connection to surrounding and preexisting bone. It was obvious that bone was more often found within the grooves than on the opposing surface of the same thread. Analyses of the implant cross sections showed that bone was present

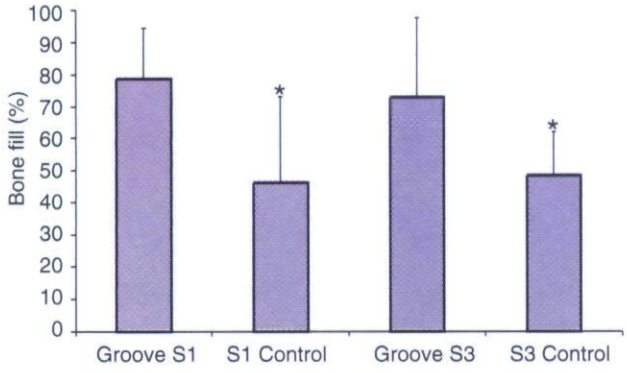

Figure 5 Graph showing bone fill in grooves and opposing surfaces as calculated for all threads.* $p < .05$

TABLE 2 Results from Histomorphometric Measurements of Tibial Specimens

Parameter	S1	C_{S1}	*p* Value
Bone area, %	13.9 ± 8.3	8.9 ± 7.6	NS
Bone contact, %	24.7 ± 16.1	20.2 ± 8.6	NS
Parameter	**S3**	**C_{S3}**	***p* Value**
Bone area, %	12.8 ± 4.1	7.0 ± 4.5	NS
Bone contact, %	26.4 ± 15.8	18.6 ± 9.9	NS

C = control.

within approximately 70% of the grooves. It is likely that the bone seen in the cross sections of the grooves was actually interconnected and that bone originating from the endosteum had been formed along the groove in the apical direction.

Bone formation depends on a continuous recruitment and differentiation of stem cells into osteoblasts. The results suggest that the physical/chemical environment within the groove increased the density of such cells. It is possible that the driving force for directed cell migration into and within the groove was a concentration gradient of chemotactic molecules. Such a gradient may have resulted from mechanical forces stimulating cellular production of such molecules. No additional load apart from forces developed during movements was applied to the implants. However, the distribution pattern of small but non-negligible mechanical forces within and in the near vicinity of the groove may have been different compared with the force distribution in the vicinity of the other surfaces of the implant. Such forces may have resulted from motion of fluids during animal movement and may have had a stimulating effect on the cellular response. It is also possible that chemotactic agents originated from the degradation process of the fibrin clot, which was likely formed within the groove shortly after implant insertion. A concentration gradient may then have been established, which allowed for cell migration along the groove.

CONCLUSION

It is concluded that 110 and 200 μm–wide and 70 μm–deep grooves at oxidized implant surfaces stimulate bone to preferentially form within and along the groove in the rabbit model. The 110 μm–wide groove was shown to increase the resistance to shear forces significantly. It is suggested that implants with such a groove may be one way to further optimize implant stability in suboptimal clinical conditions.

REFERENCES

1. Esposito M, Hirsch JM, Lekholm U, Thomsen P. Biological factors contributing to failures of osseointegrated oral implants.(I). Success criteria and epidemiology. Eur J Oral Sci 1998; 106:527–551.
2. Wennerberg A. On surface roughness and implant incorporation. Göteborg, Sweden: University of Göteborg, 1996. (Thesis)
3. Ericsson I, Johansson CB, Bystedt H, Norton MR. A histomorphometric evaluation of bone-to-implant contact on machine-prepared and roughened titanium dental implants. A pilot study in the dog. Clin Oral Implants Res 1994; 5:202–206.
4. Gotfredsen K, Berglundh T, Lindhe J. Anchorage of titanium implants with different surface characteristics: an experimental study in rabbits. Clin Implant Dent Relat Res 2000; 2:120–128.
5. Qahash M, Wikesjö UM, Thomson RC, Cook AD, Wozney JM, Hardwick WR. Surface-etching improves dental implant osseointegration in newly formed and native bone. J Dent Res 2002; 81: IADR-Abstract 4000.
6. Lima LA, Fuchs-Wehrle AM, Lang NP, et al. Surface characteristics of implants influence their bone integration after simultaneous placement of implant and GB membrane. Clin Oral Implants Res 2003; 14:669–679.
7. Hall J, Lausmaa J. Properties of a new porous oxide surface on titanium implants. Appl Osseointegration Res 2000; 1:5–8.
8. Albrektsson T, Johansson C, Lundgren AK, Sul Y, Gottlow J. Experimental studies on oxidized implants. A histomorphometrical and biomechanical analysis. Appl Osseointegration Res 2000; 1:21–24.
9. Ivanoff C-J, Widmark G, Johansson C, Wennerberg A. Histologic evaluation of bone response to oxidized and turned titanium micro-implants in human jawbone. Int J Oral Maxillofac Implants 2003; 3:341–348.
10. Zechner W, Tangl S, Fürst G, et al. Osseous healing characteristics of three different implant types. A histologic and histomorphometric study in mini-pigs. Clin Oral Implants Res 2003; 14:150–157.
11. Albrektsson T, Johansson C, Lundgren AK, Sul Y, Gottlow J. Experimental studies on oxidized implants. A histomorphometrical and biomechanical analysis. Appl Osseointegration Res 2000; 1:21–24.
12. Henry P, Tan A, Allan B, Hall J, Johansson C. Removal torque comparison of TiUnite and turned implants in the greyhound dog mandible. Appl Osseointegration Res 2000; 1:15–17.
13. Glauser R, Ree A, Lundgren A, Gottlow J, Hammerle CH, Scharer P. Immediate occlusal loading of Brånemark implants applied in various jawbone regions: a prospective, 1-year clinical study. Clin Implant Dent Relat Res 2001; 3:204–213.
14. Glauser R, Lundgren AK, Gottlow J, et al. Immediate occlusal loading of Brånemark TiUnite implants placed predominantly in soft bone: 1-year results of a prospective clinical study. Clin Implant Dent Relat Res 2003; 5(Suppl 1):47–56.
15. Glauser R, Gottlow J, Lundgren AK, Sennerby L, Portmann M, Ruhstaller P, et al. Immediate occlusal loading of Brånemark MK IV TiUnite implants placed in bone quality type 4. Appl Osseointegration Res 2002; 3:22–24.
16. Rocci A, Martignoni M, Burgos P, Gottlow J, Sennerby L. Histology of retrieved immediately and early loaded oxidized implants. Light microscopic observations after 5 to 9 months of loading in the posterior mandible of 5 cases. Clin Implant Dent Relat Res 2003; 5(Suppl 1):88–98.
17. Lundgren S, Brechter M. Preliminary findings of using oxi-

dized titanium implants in reconstructive jaw surgery. Appl Osseointegration Res 2002; 3:35–39.

18. Pilliar RM, Deporter DA, Watson PA, Todescan R. The Endopore implant-enhanced osseointegration with a sintered porous-surfaced design. Oral Health 1998; 88:61–64.
19. Ryu HS, Kim SJ, Kim JH, et al. Fabrication of 1-dimensional porous hydroxyapatite and evaluation of its osteoconductivity. J Mater Sci Mater Med 2004; 15:267–73.
20. Schüpbach P, Glauser R, Rocci A, et al. The human bone-oxidized titanium implant interface. A light microscopic, scanning electron microscopic, back-scatter scanning electron microscopic and energy-dispersive x-ray study of clinically retrieved dental implants. Clin Implant Dent Relat Res 2005;7(Suppl 1):36–43.
21. Boyan BD, Lossdorfer S, Wang L, et al. Osteoblasts generate an osteogenic microenvironment when grown on surfaces with rough microtopographies. Eur Cell Mater 2003; 6:22–27.
22. den Braber Brunette DM, Chehroudi B. The effects of the surface topography of micromachined titanium substrata on cell behavior in vitro and in vivo. J Biomech Eng 1999; 121:49–57.
23. Boyan BD, Bonewald LF, Paschalis EP, et al. Osteoblast-mediated mineral deposition in culture is dependent on surface microtopography. Calcif Tissue Int 2002; 71:519–529.
24. Davies JE. Understanding peri-implant endosseous healing. J Dent Educ 2003; 67:932–49.
25. de Bruijn JD, van Blitterswijk CA, Davies JE. Initial bone matrix formation at the hydroxyapatite interface in vivo. J Biomed Mater Res 1995; 29:89–99.
26. van Blitterswijk CA, Bakker D, Hesseling SC, Koerten HK. Reactions of cells at implant surfaces. Biomaterials 1991; 12:187–93.
27. Miranda-Burgos P, Sennerby L, Hall J. A biomechanical and histological evaluation of oxidized titanium implants with an 80, 110 or a 160 μm wide groove added to one thread flank. A study in the rabbit. (Submitted).